Core and Large Scale Structure of 2000 November 24 X-class Flare and CME

Haimin Wang, Peter Gallagher, Vasyl Yurchyshyn, Guo Yang and Philip R. Goode

Big Bear Solar Observatory, New Jersey Institute of Technology
40386 North Shore Lane, Big Bear City, CA 92314-9672

haimin@flare.njit.edu -- Version on December 14, 2001

ABSTRACT

In this paper, we present three important aspects of the X1.8 flare and the associated CME which occurred on 2000 November 24: (1) The source of the flare is clearly associated with a magnetic channel structure (Zirin & Wang, 1993), which is due to a combination of flux emergence inside the leading edge of the penumbra of the major leading sunspot and proper motion of the sunspot group. The channel structure provides evidence for twisted flux ropes which can erupt forming the core of a CME, and may be a common property of several super-active regions which have produced multiple X-class flares in the past. (2) There are actually three flare ribbons visible. The first can be seen moving away from the flare site, while the second and third make up stationary ribbon near the leader spot. The moving ribbons could be due to a shock associated with the erupting flux rope, or due to the interaction of erupting rope and the surrounding magnetic fields. In either case, the ribbon motion does not fit the classical Kopp-Pneuman model (Kopp and Pneuman, 1976) in which the separation of ribbons is due to magnetic reconnection at successively higher and higher coronal altitudes. (3) From the coronal dimming observed with EIT, the CME involved a much larger region than the initial X-class flare. By comparing high resolution full-disk Hα and EIT observations we found that a remote dimming area is cospatial with the enhanced Hα emission. This result is consistent with the recent model of Yokoyama and Shibata (2001) that some dimming areas near footpoints may be due to chromospheric evaporation.

Subject headings: Sun: activity – Sun: flares – Sun: magnetic fields – Sun: coronal mass ejection

1. INTRODUCTION

A solar coronal mass ejection (CME) represents a large-scale rearrangement of the Sun's magnetic structure which can lead to a coronal transient in the interplanetary medium. Each CME may carry away a mass of up to 10^{13} kg and release up to 10^{25} J of energy from coronal magnetic fields (Harrison 1991, 1995 and 1997). CMEs showing diffuse ring-like structure above the solar disk are name "halo" CMEs and were first reported by Howard et al. (1982), using observations made with the Solwind coronagraph on the P78-1 spacecraft. Several halo events were studied based on LASCO observations (Plunkett et al., 1998, Thompson et al., 1998; Zarro et al., 1999) on board SOHO and would seem to be more important in space weather than limb events since they can be related to the Earth-directed CMEs.

Disk coronal dimmings have been identified in association with halo events detected with the *Yohkoh* Soft X-ray Telescope (SXT, Tsuneta et al., 1991) and SOHO Extreme Ultraviolet Telescope (EIT, Delaboudinière et al., 1995), e.g. Gopalswamy and Hanaoka (1998), Sterling and Hudson (1997) and Thompson et al. (1998). These transient dimmings are often interpreted to represent the loss of the coronal mass which is swept into the CME. Wang et al. (2000) found that for the eruptions studied, the onset of dimming occurred hours before the onset of the associated flares. Therefore, flares might represent only a small part of a large scale magnetic field restructuring associated with CMEs.

Several authors including some from our group have recently paid attention to the large scale structure of CMEs, including eruptions from interconnecting active regions (Wang et al. 2001), and transequatorial loops (Pevtsov 2000), which connect two active regions in opposite hemispheres. The large scale dimming (Wang et al., 2000, Thompson et al., 1998) is another important hint for the large scale structure of CMEs.

In this paper, we report the detailed analyses of one of four X-class flares that occurred between November 24 and 26, 2000, in AR9236. We studied the source region of the flare as well as the large coronal structure associated with this flare. As all the four flares showed very similar morphologies in soft and hard X-ray observations, the physical picture discussed here based on one event may actually represent all four events.

2. OBSERVATIONS AND DATA REDUCTION

For this study, the data was obtained from the following sources:

(1) BBSO full disk Hα movies. The cadence was 1-minute and the pixel resolution was $1''$.

(2) BBSO digital magnetograms (DVMG), which covers an area of about 300″ by 300″. This new system has a much improved sensitivity and resolution compared to that of the old BBSO videomagnetograph system (Spirock et al. 2001). However, only line-of-sight magnetograms were obtained on this day.

(3) EIT FeXII 195Å full disk observations. EIT provides full-disk images of the corona and transition region extending to 1.5 solar radii above the solar limb. It observes in 4 spectral bands centered on: FeIX/X (171 Å), Fe XII (195 Å), Fe XV (284 Å) and He II (304 Å). These lines allow imaging of solar plasma at temperatures ranging from 6×10^4K to 3×10^6K (Delaboudinière et al. 1995). On November 24, 2000, only FeXII 195Å data were obtained continuously. The cadence was 15 minutes, and pixel resolution was 2.5″. The sensitivity of this line peaks at between 1 and 2×10^6K.

(4) LASCO data. We were especially interested in the C2 and C3 white-light data for CMEs. C2 and C3 are two externally occulted instruments. C2 covers the range of 2 to 6 solar radii and C3, 4 to 32 solar radii (Brueckner et al. 1995). The cadence for our observations was 24 minutes.

(5) Full-disk MDI magnetograms. MDI mainly obtains full-disk Dopplergrams, for the investigation of solar oscillations. However, it can obtain magnetograms of various cadences and image sizes (Scherrer et al., 1995). For the data used in the current study, the cadence was 90-minutes, with an image scale of 2″.

(6) *Yohkoh* HXT and SXT data were used to identify flare kernels and loops.

3. RESULTS

3.1. Evolution of the Magnetic Field

It is well known that emerging flux regions (EFRs) are closely associated with solar flares and the onset of CMEs (e.g., Feynman & Martin 1995). This new flux emergence may perturb the existing magnetic configuration above the solar surface and thus, trigger a CME. It has also been found that a complicated flow pattern on the solar surface may actually result from the emergence of twisted flux tubes (Tanaka 1991). Zirin & Wang (1993) also discovered that magnetic flux can emerge inside the penumbrae of existing sunspots. This kind of new flux emergence can produce a so-called magnetic channel, which is an elongated magnetic structure with alternating magnetic polarities and strong transverse magnetic fields along the channels (see e.g., Figure 3). Surface plasma flows are observed along the channels as well. The penumbral flux emergence is also known to be a common property of a few

super-active regions, which produced multiple major solar flares, such as NOAA 5395 in March 1989, NOAA 6659 in June 1991, and NOAA 9393 in March/April 2001. The channel swept around the leading sunspot, likely due to fast proper motion of the spot in the leading direction.

The evolution of NOAA AR 9236 in November 2000 gives a very clear example of flux emergence inside existing penumbra and the formation of the channel structure. Figure 1 shows a series of magnetograms obtained with the MDI instrument from November 23 till November 26. The flux emergence occurred at the leading edge of a well-defined leading sunspot. The new flux accumulated in two areas: area N collected negative flux, while positive flux was collected in area P.

Figure 2 plots the total positive and negative flux of the active region. The new flux emergence is clearly demonstrated in the plot. The negative flux increased about 1.5×10^{21} Mx, mainly from the mid-day of November 23 to the end of November 24. The positive flux increased 4.6×10^{21} Mx. We believe that the negative flux increase is an accurate account of new flux, as part of the positive flux increase is due to the geometric effect: the region was rotating towards the disk center, therefore, the main sunspot flux would increased even without new flux. This effect was particularly obvious in the first 12 hours of November 24, when there was no flux increase in the negative polarity. The bottom panel of Figure 2 shows corresponding GOES X-ray plot for the 3-day period. Three X-class flares occurred during the flux building period (12UT November 23 to 00UT November 25). The last X-class flare occurred on November 26, when the flux ceased to increase. The vertical bar in the upper panel marked the X1.8 flare, studied in this paper.

Figure 3 shows a BBSO magnetogram at 18:43 UT, 3 hours before the flare. The rectangle encloses the center part of the emerging flux, where we identified an elongated channel structure which corresponds to the area "A" in Figure 1. This structure is characterized by alternating positive and negative magnetic polarities, the width of each channel is between 5 to 10 arcsec. The right panel in Figure 3 shows an Hα image of the flare at 21:50 UT, where the channel structure is located in the core of the flare. A *Yohkoh* hard X-ray image in the M1 channel is over-plotted as contours in the Hα image. Two kernels are clearly visible, which will be discussed later. Please note that, because of the nature of the magnetic channel (mixed polarity in very small scale), it only shows during the best observing period in a day with excellent seeing.

3.2. Flare Ribbons

Figure 4 shows the evolution of the flare in Hα. There are three Hα brightenings located "A", "B" and "C" in the figure. An initial glance at a flare movie would treat brightenings "A" and "B" as two conjugate ribbons, with brightening "B" moving away from the sunspot, as the flare progresses. It became apparent after careful study that the brightening "A" consists of two unresolved flare ribbons, as evidenced by two hard X-ray kernels marked with "K1" and "K2". Initiation of "A" is clearly associated with an erupting flux rope "F" (Figure 3). This flux rope, or possibly filament, is located near the neutral line of the magnetic field that divides two unresolved ribbons within brightening "A". However, it also may be a flux rope itself representing the flux emergence as discussed in the previous section. Flare ribbon "B" propagates outward, away from the sunspot and the flare core, at a speed of about 50 km s^{-1}. The speed and the direction of the motion of the flare ribbon "B" agree with those of erupting flux rope "F". It may be due to two possible mechanisms: (1) The erupting flux rope created a shock front and the projection of the shock onto the chromosphere is seen in the form of a moving flare ribbon "B". (2) The erupting flux rope interacts with outlying coronal loops, and reconnection occurs higher up in the corona. Then, as a result of such reconnection, the moving flare ribbon "B" formed by particles traveling along the field lines and precipitation into the chromosphere. This is illustrated by the cartoon in Figure 5. Explanation (2) may be more reasonable, because the propagation of ribbons basically follow the pattern of magnetic network elements, indicating electron precipitation along magnetic field lines.

3.3. EUV Dimmings and Hα Remote Brightening

The remote brightening "C" seen in the Hα images (Figure 4) is also of interesting. Traditionally, researchers concentrated on high-resolution Hα observations with limited field-of-view, so that we might have overlooked what happened outside flaring active regions. High quality full-disk from BBSO enables us to study areas in close proximity to a solar flare and/or an active region, and therefore, to understand the large scale morphology of a solar flare and the associated CME. In Figure 6, we compare two difference images. The top-left panel gives an Hα difference image created by subtracting an image taken at 21:53 UT from an image at 21:05 UT. The top-right panel shows coronal dimmings in an EIT difference image at 23:36 UT subtracted by a preflare image at 20:00 UT. Care was also taken to differentially rotate all frames to 21:00UT before subtract. The coronal dimming associated with the remote Hα brightening "C" is clearly visible. The bottom-left panel shows a MDI magnetogram at 20:48 UT for comparison. Flare kernels "B" and "C", appearing in Figure

4, are located in opposite polarity magnetic fields and might be conjugate points connected by the disturbed field lines (Figure 5). The bottom-right panel compares a SXT image, showing a very faint loop connecting "B" and "C". The association between the EIT dimming and the Hα remote brightening may give one possible reason for a coronal dimming to occur: chromospheric evaporation at a flare site which reduces the coronal density just above the footpoints. When the released energy is transported from the reconnection site to the upper chromosphere, the plasma there is suddenly heated to form a localized high pressure region. The induced pressure-gradient force drives the dense plasma to flow up toward the corona along the field line. This backward upflow process is called chromospheric evaporation (Neupert, 1968; Hirayama, 1974; Antiochos & Sturrock, 1978; Canfield & Gunkler, 1985, Silva et al., 1997). Recently, Yokoyama and Shibata (2001) developed 2-D MHD model and found the relationship between the dimming and flare. Cospatial of dimming and footpoint brightening in Figure 6 provides the evidence that the density near the footpoint is reduced due to the evaporation, which transports material to the loop top. Clearly, this kind of dimming is different from wave associated dimming (Harra and Sterling, 2001), which also has strong upward Doppler signature. We need to point out two limitations of this study (1) Without comparing the evolution of the dimming with spectroscopic measurements of Hα redshifts and/or soft X-ray blueshifts, one cannot make the claim that dimming and evaporation are physically connected. We do not have such data set available. However, we just provide evidence of this possible connection, without claiming the the connection. The evidence is that we see dimming near the footpoint, not the loop top. What we can state is that there is observational evidence to support the model of Yokoyama and Shibata (2001). (2) The evaporation, if exists, only can explain a small portion of the dimming, and the majority of the dimming is due to the erupting material which becomes part of the CMEs.

4. SUMMARY

From our study, we found three important aspects of this event:

(1) The source region of the flare is clearly associated with the magnetic channel structure, caused by flux emergence within the leading edge of the penumbra of the major leading sunspot in the sunspot group. The channel structure provides evidence of the eruption of entangled ropes being the core of the flare. This evidence leads us to the conclusion that this kind of flux emergence is the generic property of super-active regions which produced multiple X-class flares.

(2) Careful study shows that there are actually three flare ribbons: The stationary ribbon "A" is a flare core, and it consists of two unresolved ribbons. The third moving

ribbon "B" could be due to a shock induced by erupting flux rope, or alternatively, could be due to the interaction of the erupting flux rope with the surrounding coronal magnetic loops. In either case, the motion of the ribbon does not fit the classical Kopp-Pneuman model, where the separation of flare ribbons is due to magnetic reconnection at progressively higher coronal altitudes.

(3) Evident from the extended dimming, the flare associated CME involved magnetic structures of much larger spatial scales than the flare source region. From high-resolution full-disk Hα and EIT data we found that the remote dimming is associated with a weak Hα emission. This provides evidence that this remote dimming may be due to evaporation of the chromospheric material heated by the flare. So the emission measure near the footpoint is reduced. However, this mechanism only explains a small fraction of dimmings.

We are grateful to the BBSO observing staff for their support in obtaining the data. We thank the referee for very valuable comments which improved the paper significantly. The work is supported by NSF under grants ATM-0076602, ATM-9903515 and ATM-0086999, NASA under grants NAG5-9682, NAG5-9738 and NAG5-10910, and ONR under grant N00014-97-1-1037.

REFERENCES

Antiochos, S. K. & Sturrock, P. A. 1978, Ap. J., 220, 1137

Brueckner, G.E. & 14 others, 1995, Solar Physics, 162, 357

Canfield, R. C. & Gunkler, T. A. 1985, Ap. J., 288, 353

Delaboudinière, J.P., & 28 others, 1995, Solar Physics, 162, 291

Feynman, J & Martin, S.F., 1995, JGR, 100, 3355

Gopalswamy, N. & Hanaoka, Y., 1998, Ap. J. Letters, 498, L179

Gopalswamy, N., Nitta, N., Manoharan, P.K., Raoult, A. & Pick, M., 1999, A&A, 347, 684

Harra, L. K. & Sterling, A.C., 2001, Ap. J. Letters, 561, L215

Harrison, R.A., 1991, Philosophical Transactions of Royal Society of London, 336, 401

Harrison, R.A., 1995, Astron. and Astrophys., 304, 585

Harrison, R.A., 1997, 'Overview of Results from IACG Campaign 3: CME Onsets', ESA SP-415, 121

Hirayama, T. 1974, Solar Physics, 34, 323

Howard, R.A., Michels, D.J., & Sheeley, N.R., Jr., 1982, Ap.J. Letters, 263, L101

Kopp, R. A & Pneuman, G.W., 1976, Solar Physics, 50, 85

Neupert, W. M. 1968, Ap. J., 153, L59

Pevtsov, A.A., 2000, Ap. J., 531, 553

Plunkett, S.P, Thompson, B.J., Howard, R.A., Michels, D.J., St. Cyr, O.C., Tappin, S.J., Schwenn, R. & Lamy, P.L., 1998, Geophysical Research Letters, 25, 2477

Scherrer, P.H. & 12 others, 1995, Solar Physics, 162, 129

Silva, A. V. R., Wang, H., Gary, D. E., Nitta, N. & Zirin, H. 1997, Ap. J., 481, 978

Spirock, T. J., Denker, C., Varsik, J., Shumko, S., Qiu, J., Gallagher, P., Chae, J., Goode, P. & Wang, H., 2001, AUG Summer Meeting, Boston, SP51B06

Sterling, A. & Hudson, H.S., 1997, Ap. J. Letters, 491, L55

Thompson, B.J., Plunkett, S.P., Gurman, J.B., Newmark, J.S., St. Cyr, O.C., & Michels, D.J., 1998, Geophysical Research Letters, 25, 2465

Tanaka, K., 1991, Solar Physics, 136, 133

Tsuneta et al., 1991, Solar Physics, 136, 37

Wang, H., Goode, P., Denker, C., Yang, G., Yurchyshyn, V., Nitta, N., Gurman, J.B. & St. Cyr, C., 2000, Ap.J., 536, 971

Wang, H., Chae, J., Yurchyshyn, V., Yang, G., Steinegger, M. & Goode, P.R., 2001, Ap.J., 559, 1171

Yokoyama, T. & Shibata, K., 2001, Ap.J., 549, 1160

Zarro, D.M., Sterling, A.C., Thompson, B.J., Hudson, H.S. & Nitta, N., 1999, Ap. J. Letters, 520, L139

Zirin, H. & Wang, H., 1993, Nature, 363, 426

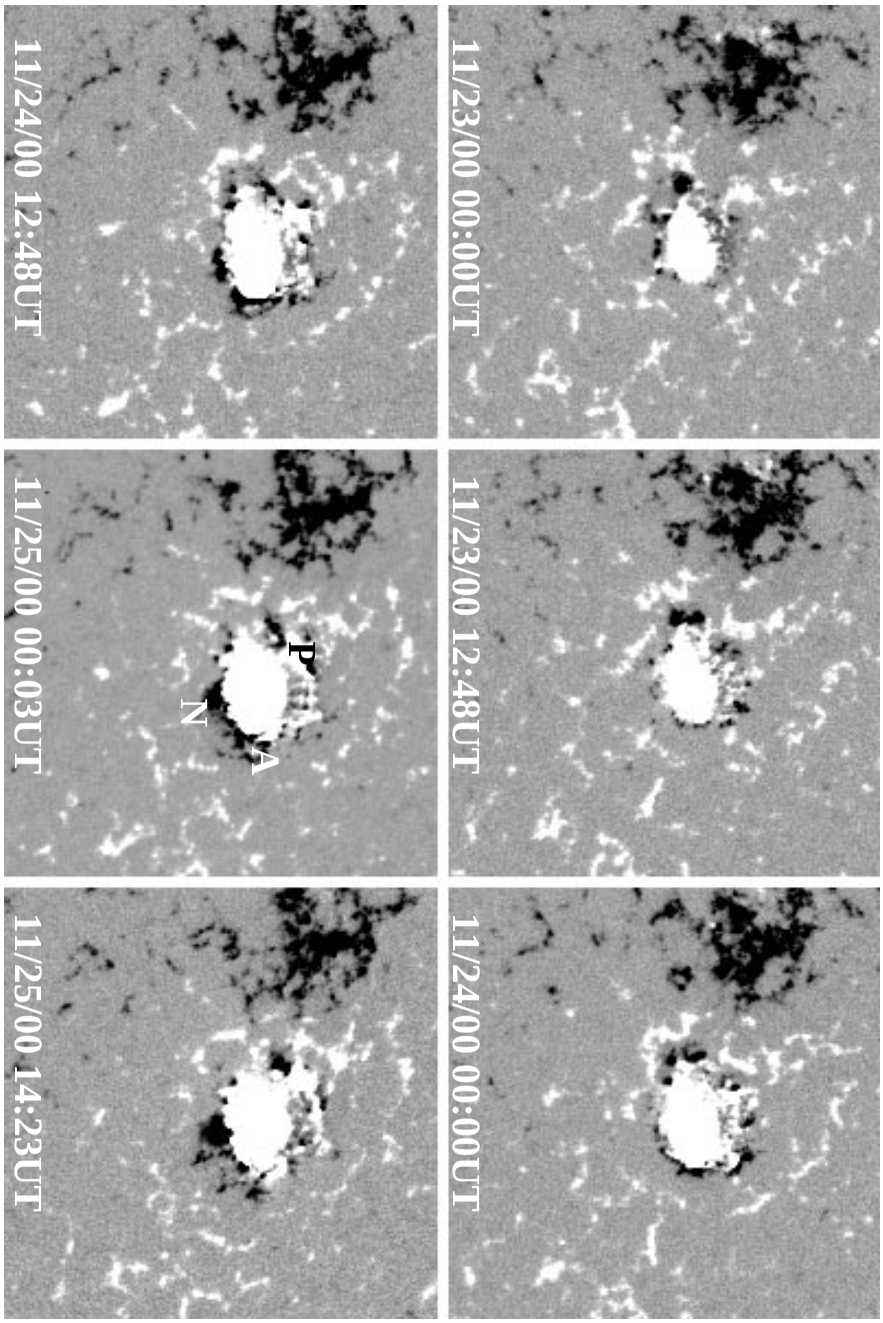

Fig. 1.— A sequence of MDI magnetograms from November 23 till November 25, 2000. The field-of-view is 400×400 arcsec. The "A" denotes the location of the beginning of the flux emergence. Negative polarity magnetic flux accumulates at "N", while positive magnetic flux accumulates at ″P".

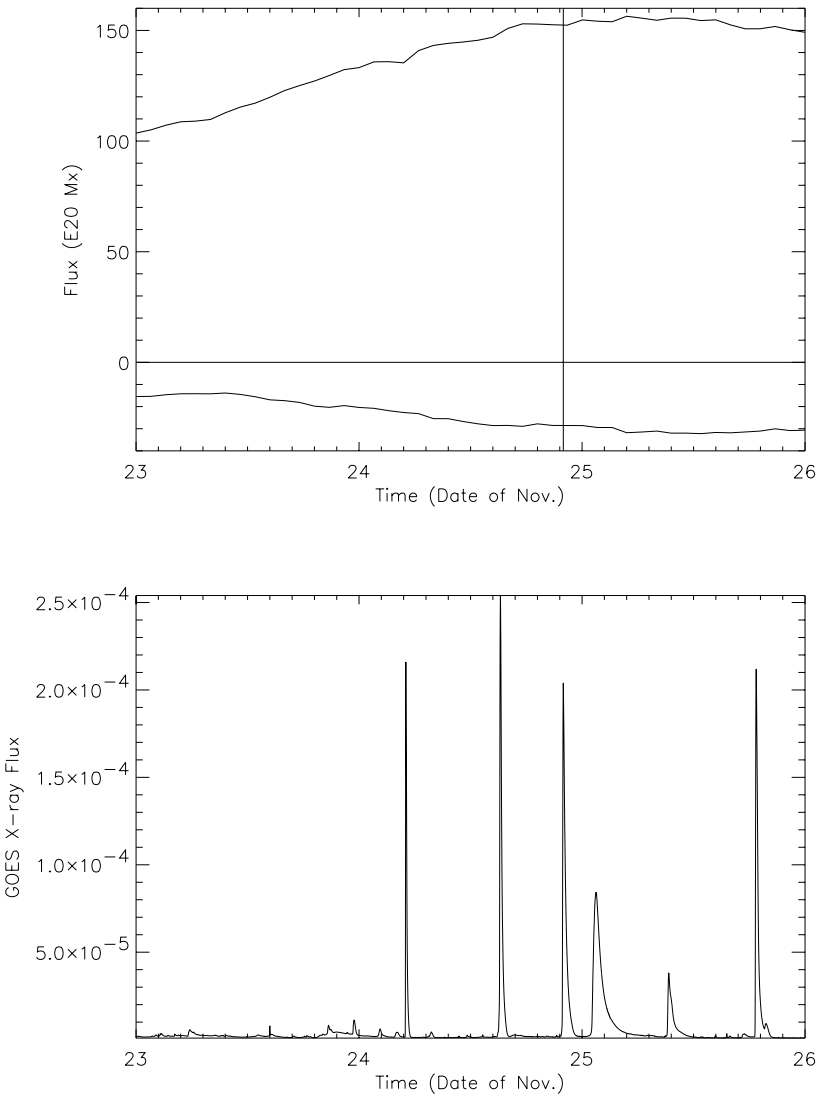

Fig. 2.— Top panel: plot of positive and negative of magnetic fluxes in the active region as a function of time. The vertical bar denotes the time of the X1.8 flare studied in this paper. Bottom panel: GOES X-ray flux (Watts/m^2) as a function of time in the softer channel (1 to 8Å). Four X-class flares occurred during this three-day period.

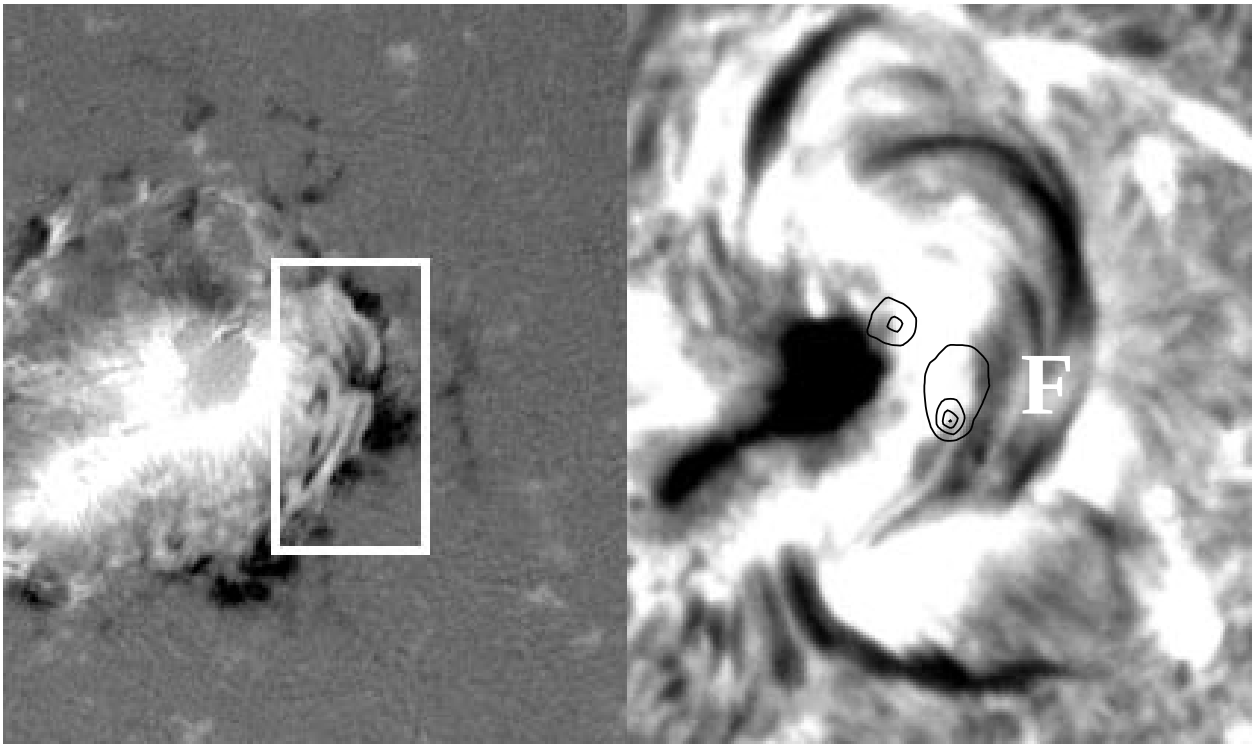

Fig. 3.— Comaprison of a high resolution BBSO DMG magnetogram (left) with an Hα flare image (right). The white rectangle marks a magnetic channel structure. The field-of-view is 150×180 arcsec. A flux rope is denoted with "F".

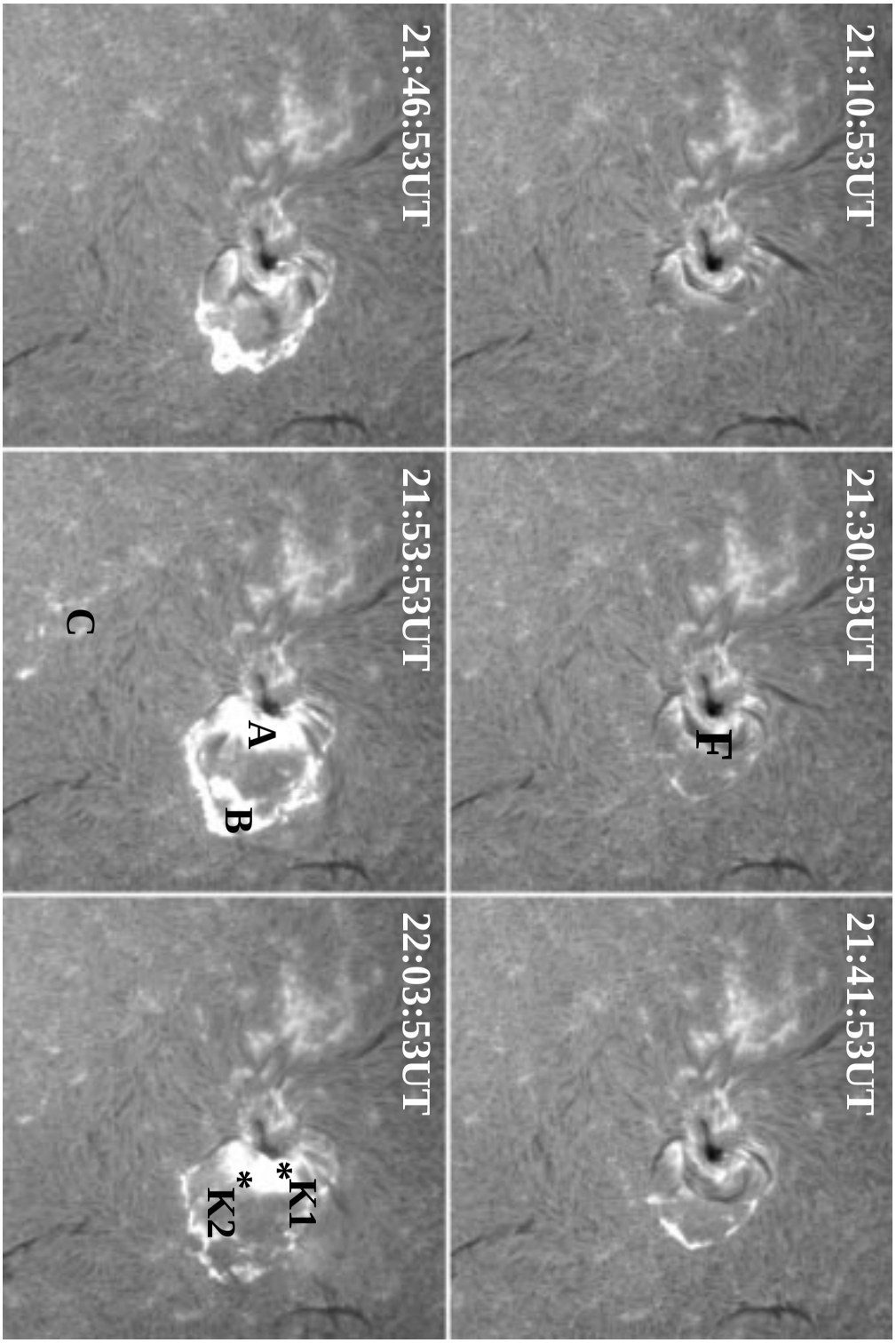

Fig. 4.— A sequence of Hα subframes from BBSO full-disk images showing the evolution of the active region during the flare. The field-of-view is 600×600 arcsec. Hα flare kernels are denoted by "A" and "B", while "K1" and "K2" mark the location of two hard X-ray kernels. A remote brightening is denoted by "C".

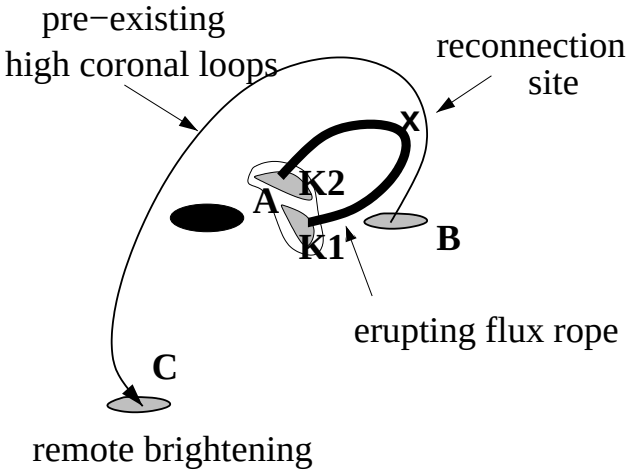

Fig. 5.— A cartoon illustrating the interaction between the erupting rope (thick line) and the pre-existing higher coronal loop (thin line). The reconnection created both flare ribbon "B" and remote brightening "C".

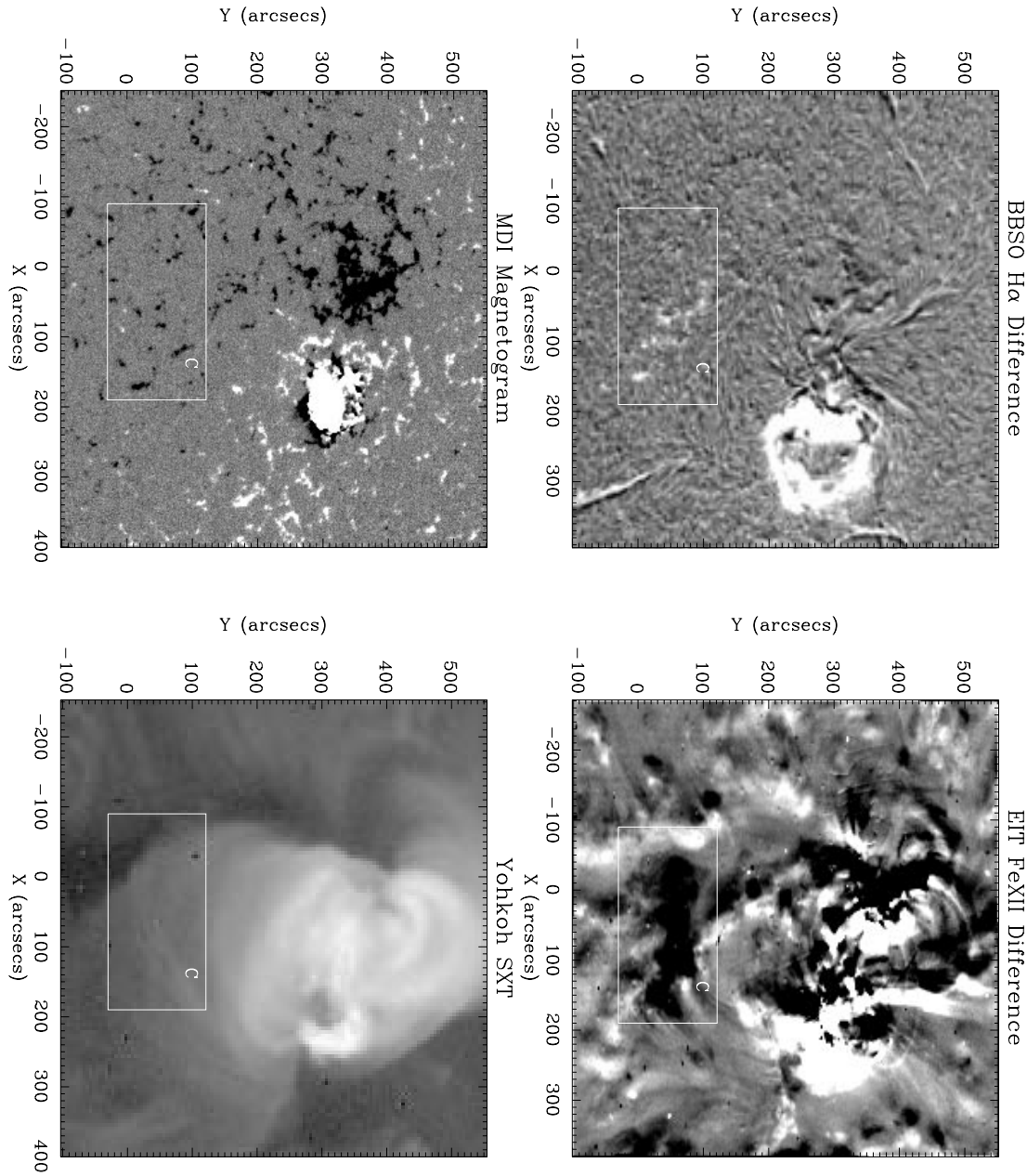

Fig. 6.— Hα and EIT difference images. The remote brightening "C" is associated with a dimming, marked by the white box. The bottom panels compare a MDI magnetogram and a Yohkoh SXT image in the same field of view.